

DE GRUYTER
OPEN

ARCHIVES OF MECHANICAL TECHNOLOGY AND MATERIALS

WWW.AMTM.PUT.POZNAN.PL



The numerical investigation of thin-walled beams with modified C-sections

Michał Grenda^{a*}

^a Poznan University of Technology, Division of Strength of Materials and Structures, Institute of Applied Mechanics, 60-965 Poznan, Poland

*Tel.: +48-660-961-749, e-mail address: michal.wl.grenda@doctorate.put.poznan.pl

ARTICLE INFO

Received 05 February 2018
Received in revised form 27 July 2018
Accepted 19 September 2018

KEY WORDS

Thin-walled, FSM, numerical investigation, Finite strip method, C-sections, cold-formed,

ABSTRACT

Demand for thin-walled structures has been increasing for many years. Cold-formed, thin-walled channel beams are the subject of presented research. The local elastic buckling and limit load of these beams subjected to pure bending are investigated. This study includes numerical investigation called the Finite Strip Method (FSM). The presented results give a deep insight into behaviour of such beams and may be used to validate analytical models. The number of works devoted to the theory of thin-walled structures has been steadily growing in recent years. It means that is an increasing interest in practical methods of manufacturing cold-formed thin-walled beams with complicated cross-sections, including also beams with web stiffeners. The ratio of transverse dimensions of beam to its wall-thickness is high, therefore, thin-walled beams are prone to local buckling that may interact with other buckling modes. The stability constraints should be always considered when using cold-formed thin-walled beams.

1. INTRODUCTION

Thin-walled cold-formed steel beams with open cross-section have become more and more common structural elements which are used in a wide range of applications: civil engineering, automotive industry, aviation, vessel industry and railway industry. Their cross-sections may have complicated shapes that can be made thanks to the development in manufacturing and material technologies. Those shapes make it possible to improve the stiffness and load capacity of beams without increasing their weight. Therefore, parameters describing cross-sections should be calculated by solving mathematical optimization problems. Cold-forming technology has many advantages:

- less energy is needed during forming processes than for example for hot formed technology or section rolling,
- it is cheaper than traditional technologies,
- it can be used for sheet metals covered by anticorrosive coatings.

However, thin-walled beams have also some disadvantages. They can be easily damaged if working

parameters change even not too much. Their load capacity and strength may be affected by small inaccuracies (material parameters, loading and working conditions, geometrical imperfections).

In this paper, the authors have investigated some thin-walled cold-formed channel beams subjected to pure bending.

Ungureanu and Dubina [1] analysed the influence of imperfections on the behaviour of perforated pallet rack members in compression using non-linear FE simulations. The effect of imperfections, perforations and buckling modes reduces significantly the capacity of perforated members in compression, especially in the coupling range due to interaction. Rasmussen and Hancock [2] proposed numerical models to generate automatically the geometrical imperfection modes into the non-linear analysis. Sudhir Sastry et al. [3] conducted the lateral buckling analysis of cold-formed thin-walled beams subjected to pure bending. Critical buckling loads were estimated using optimization criteria and compared with published results. Bienias et al. [4] presented the post-buckling analysis and calculated load carrying capacity of thin-walled composite channels

DOI: 10.2478/amt-2018-0010

© 2018 Author(s). This is an open access article distributed under the Creative Commons Attribution-Non Commercial-No Derivs license (<http://creativecommons.org/licenses/by-nc-nd/3.0/>)

Brought to you by | Politechnika Poznanska - Poznan University of Technology
Authenticated

Download Date | 11/30/18 1:04 PM

subjected to uniform compression using FEM and ANSYS software. Chen et al. [5] showed the investigations of web crippling behaviour of cold-formed steel lipped channel beams subjected to end-one-flange (EOF), interior-one-flange (IOF), end-two-flange (ETF), and interior-two-flange (ITF) loading conditions. They tested 48 cold-formed steel lipped channel beams and considered different boundary and loading conditions, bearing lengths and section heights. Experimental investigations, distribution of stresses and displacements of cold-formed thin-walled beams were presented by Paczos and Magnucki [6] and Belingardi and Scattina [7]. The other works on this subject were Biegus et al. [8], Paczos and Wasilewicz [9], Mahendran and Jeyaragan [10]. Comparison of theoretical results with experimental ones helps to improve mathematical models of beams. Such approach was taken by e.g. Magnucka-Blandzi and Magnucki [11], who also prepared a review of papers on steel cold-formed structures. Similar problems were analysed by other research and some results in this field were presented by Magnucka-Blandzi et al. [12] and Paczos et al. [13-15]. They showed their own experimental and numerical investigations of thin-walled channel beams with non-standard cross-sections. Experimental investigations of thin-walled composite beams were presented by Debski, Kubiak, Teter [16] and Kołakowaki, Mania [17].

Loughlan et al. [18] analysed the stability of compressed lipped channels. They considered interaction between local and distortional buckling. Their model included material yielding and yield propagation to ultimate conditions and then to elastic-plastic unloading. Moreover, geometric imperfections were considered in numerical simulations. Luo et al. [19] presented two computational models used for analysis of distortional critical stresses of cold-formed thin-walled inclined lipped channel beams subjected to bending about the minor axis. They used Generalised Beam Theory (GBT).

Camotim and Dinis [20] and Silvestre et al. [21] tested beams subjected to pure bending, point load and uniformly distributed load. Moreover, they gave formulas to calculate critical loads including interaction between local and global buckling. The strength and stability of thin-walled beams was also considered by Trahair [21]. Contemporary analytical studies, FEA and experimental investigations of such problems were presented by Adany et al. [21]. The optimal design of thin-walled beams was discussed in details by Magnucki, Rodak and Lewiński [21], Loughlan and Yidris [25]. Optimal shapes of open cross-sections were searched by Magnucka-Balndzi, Magnucki, Monczak [21] and Maćkiewicz [28].

The presented work is a part of research that has been conducted at the Division of Strength of Materials and Structures of Poznan University of Technology. This is a part of broader research on thin-walled beams and search for new shapes of cross-sections that would increase the strength and stability of beams. The considered beams are loaded with bending moments and analysed pure bending (Eurocode3 [29]). The paper concerns non-standard, thin-walled beams with stiffened flanges made of a cold-rolled steel sheet (Fig. 1). These analysis help to verify constantly developed the Finite Strip Method and in future the finite elements method and test stands.

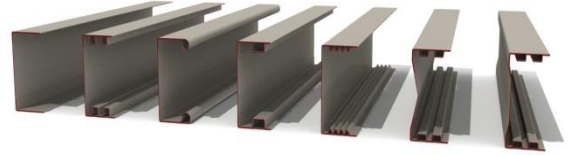


Fig. 1. The cross-sections of thin-walled channel beams

2. DESCRIPTION OF THE INVESTIGATED CROSS-SECTIONS

2.1. Geometrical properties

In numerical analyses the length L is 400, 500 and 600 mm. In the actual beams the length L is equal to 500 mm. Normal stresses at the center of the upper flange (top steel sheet) are equal to

$$\sigma_g = \frac{M_g}{J_y} \cdot \frac{H-t}{2}. \quad (1)$$

where J_y is the moment of inertia of the beam's cross-section. Pure bending is simulated by four-point bending test in which the endings of a beam is stiffened with steel sheets having better strength properties than beam. The beam loading scheme and the longitudinal dimensions of beam is shown in Fig. 2.

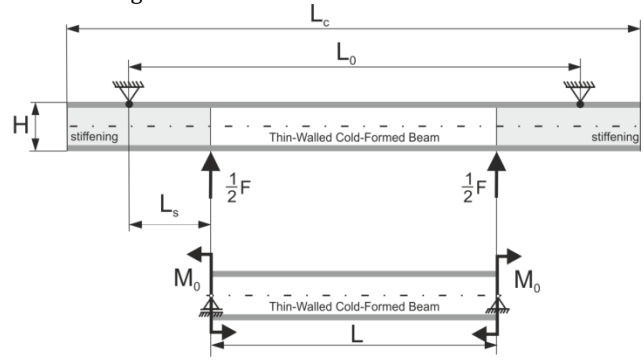


Fig. 2. Beam loading scheme and longitudinal dimensions of beam

The bending moment in the middle span may be calculated in the following way

$$M_g = \frac{1}{2} F L_s. \quad (2)$$

After basic transformations and putting equation (2) in (1) the relationship between loading force and stresses is

$$F = \frac{4J_y \sigma_g}{(H-t)L_s}. \quad (3)$$

The subjects of the investigation are non-standards thin-walled channel C-beams. Thin-walled beams with open cross sections are used in mechanical and civil engineering.

The investigated thin-walled channel beams have unconventional cross-sections therefore, the following nomenclature for denoting them is introduced:

- Beam B1 –lipped flanges without stiffened web,
- Beam B2 – lipped flanges with perforated web,

- Beam B3 – sigma,
- Beam B4 – sigma with perforated web (DBFB-B4),
- Beam B5 – double box flanges and stiffened web (DBFB-B5).

The dimensions of beams are presented in Fig. 3.

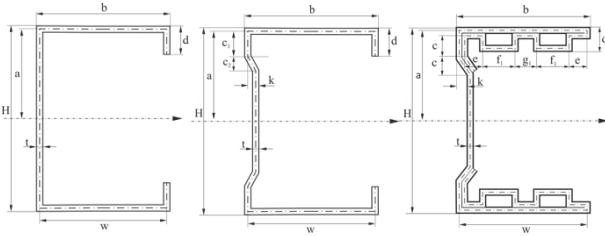


Fig.3. Analysed beams: the dimensions of cross-sections

Tab. 1. Geometric properties and the dimensions of beams

Geometric Properties	Symbol	Dimensions
The depth of beam	H	160 mm
The width of flange	b+t	80 mm
The wall-thickness	t	0.6 – 3.0 mm
The total length of beam	L_c	2000 mm
The length of the middle span	L	400, 500, 600 mm
The distance between supports	L_0	1960 mm
The length of stiffeners	L_s	780, 730, 680 mm
The length of lips	d	26.5 mm
The height of flanges	d	17 mm
The distance	e	14 mm
The width of boxes	f	18 mm
The distance between boxes	g	14 mm
The distance	k	5-50 mm

The results, i.e. critical forces and stresses and respective buckling modes obtained using the Finite Strip Method, are compared and presented in tables and figures in the next paragraphs. The number of half-waves depending on the shape of cross-section, web stiffeners and wall-thicknesses are also compared. The beams were loaded by a bending moment constant along the whole beam. Beams B1 and B2 consist of 20 elements and 21 nodes and they are loaded in such a way that actual critical forces are equal to calculated load factors multiplied by 100. Some calculations were repeated by doubling and quadrupling the number of strips to check numerical results. Naturally, the best results were achieved when beams B3, B4 and B5 consisted of about 120 strips. However, the total time of calculations and differences between results are also considered. The number of elements and nodes are depending also on shape of the cross-section of the thin-walled channel beams. Basic properties of the cross-section are shown on the cross-sections (Fig. 3.).

Longitudinal boundary conditions can be set in the finite strip model. Modeling classic problems requires using feature simply supported plate. The degrees of freedom are free along its longitudinal edge and have been supported by changing the appropriate parameters. All models are simply supported at the ends due to the choice of shape function in the finite strip method. Finite strip analysis requires that you enter in a reference longitudinal stress. The buckling load factor output is a multiplier times this reference stress. The

tools in the program make entering in the reference stress easier. Based on the loads you check off, a stress distribution is generated.

2.2. Material properties

The investigated beams were made of steel sheets. Their material properties were following: Young’s modulus $E=181\text{GPa}$, Poisson’s ratio $\nu=0.3$ and yield strength $\sigma_{eH}=329\text{MPa}$. They were determined by testing 5 samples prepared according to Eurocode 3.

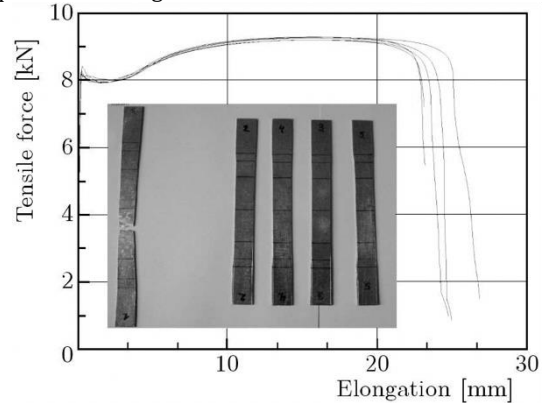


Fig. 4. The stress-strain curve of specimens – steel DX51 [14]

The results of tensile tests were presented in Fig.4. The specimens were made of steel DX51, hot-dip galvanized, zinc coating 200 g/m². These findings made it possible to determine material properties that were used in numerical analyses and analytical models.

3. NUMERICAL ANALYSIS - FSM

3.1. FSM analysis

In order to better understand the buckling of the investigated beams, numerical analyses were done. The beams were analysed using the FSM (the Finite Strip Method). In recent years, there have been a few significant works devoted to this method. Adany and Schafer [23] presented a method for calculating critical loads of thin-walled beams based on the Finite Strip Method (FSM). They made the decomposition of buckling modes using Generalized Beam Theory (GBT) that helps distinguish them from each other. Li and Schafer [31] showed another way to determine elastic critical loads used for calculating limit loads in Direct Strength Method (DSM). They proposed calculating the values of those forces that agreed with the values obtained using standard FSM for the lengths of half-waves derived from cFSM for pure buckling modes. The reason of this new approach was the lack of unambiguous minima for local and distortional buckling modes. At the end, the authors compared the new method of calculating limit loads using DSM with standard ones and another proposed by Beregszászi and Ádány [32]. Adany et al. [33] presented a method for determining buckling modes using cFSM and implemented in software CuFSM.

Djafour et al.[34] improved the constrained the finite strip method by simplifying the derivation of the constraint matrix in the case of combined global and distortional

buckling modes. This led to a simple and systematic formulation which allowed the cFSM to compute pure buckling modes for members with open and closed thin-walled cross-sections.

Chu et al. [35] investigated local stability of cold-formed thin-walled Z-channels with stiffened flanges using the Finite Strip Method. They considered simply supported beams subjected to uniformly distributed load. The obtained results were compared with previous analyses of beams subjected to pure bending. They concluded that critical moment was higher for the first load case, but difference between critical forces became smaller for longer beams.

The ratio of wall-thickness to transverse dimensions of cold-formed thin-walled beams is small. Therefore, their load capacity is usually limited by stability. Magnucka and Paczos [36] presented analytical solutions for thin-walled nonstandard channels. They validated and compared theoretical results (critical forces and buckling modes) with numerical ones using the Finite Strip Method. Paczos [14] conducted a stability analysis of channel beams with boxed flanges using CuFSM and compared the obtained results with actual experiments. The considered beams are made of cold-rolled steel sheets (Fig. 3.). CuFSM ver. 4.05 software (B. Schafer [37]) that is based on the Finite Strip Method was used for numerical analyses. New method of design thin-walled members, i.e. Direct Strength Method implemented in open source code of FSM was presented by Schafer [38].

3.2. The analysis of beam B1 – lipped flanges

The cross-section of beam B1 is presented in Fig.5. The lipped flanges improve the load capacity, strength and stability of beam without increasing its weight too much. It is typical cross-sections of C-beam which are used in a wide range of applications in civil engineering and industry.

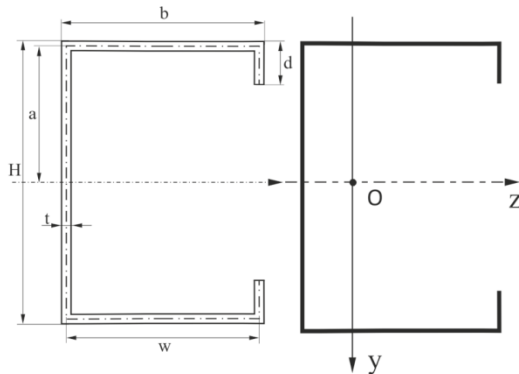


Fig. 5. The cross-section of beam B1– lipped flanges

The moment of inertia of beam B1 is equal to $J_y=92.8 \text{ cm}^4$ for the wall-thickness $t=0.6 \text{ mm}$, $J_y=123.8 \text{ cm}^4$ for the wall-thickness $t=0.8 \text{ mm}$, $J_y=154.7 \text{ cm}^4$ for the wall-thickness $t=1.0 \text{ mm}$, $J_y=170.2 \text{ cm}^4$ for the wall-thickness $t=1.1 \text{ mm}$, $J_y=185.7 \text{ cm}^4$ for the wall-thickness $t=1.2 \text{ mm}$, $J_y=194.5 \text{ cm}^4$ for the wall-thickness $t=1.25 \text{ mm}$, $J_y=232.1 \text{ cm}^4$ for the wall-thickness $t=1.5 \text{ mm}$, $J_y=309.5 \text{ cm}^4$ for the wall-thickness $t=2.0 \text{ mm}$, $J_y=386.9 \text{ cm}^4$ for the wall-thickness $t=2.5 \text{ mm}$ and $J_y=464.3 \text{ cm}^4$ for the wall-thickness $t=3.0 \text{ mm}$, respectively. The relationship between the load factor and length of half-wave and buckling mode of beam B1 (FSM) is shown in Fig. 6.

The calculated values of critical stresses/forces and the number of half-waves are presented in Tab. 2. The wall-thickness increases the values of critical loads. In addition, the dimensions of the length of the middle span L section of the cross-section of the beams tested did not significantly affect the critical stress value or the half-wave number. As mentioned earlier, five different shapes of cross-sections - three without perforated web and two with perforated web are considered (Fig. 3) and ten different wall-thicknesses (Tab. 2).

Tab.2. Beam B1, wall-thickness from $t=0.60 \text{ mm}$ to $t=3.00 \text{ mm}$: critical stresses and forces and the number of half-waves

L[mm]	400	500	600
wall-thickness	t = 0.6 mm		
σ_{cr} [MPa]	53	48	46
F_{cr} [kN]	1.6	1.5	1.6
wall-thickness	t = 0.8 mm		
σ_{cr} [MPa]	95	85	81
F_{cr} [kN]	3.8	3.6	3.7
wall-thickness	t = 1.0 mm		
σ_{cr} [MPa]	147	134	127
F_{cr} [kN]	7.3	7.1	7.2
wall-thickness	t = 1.1 mm		
σ_{cr} [MPa]	178	163	155
F_{cr} [kN]	9.8	9.5	9.7
wall-thickness	t = 1.2 mm		
σ_{cr} [MPa]	212	193	183
F_{cr} [kN]	12.7	12.3	12.5
wall-thickness	t = 1.25 mm		
σ_{cr} [MPa]	230	209	200
F_{cr} [kN]	14.4	13.8	14.2
wall-thickness	t = 1.5 mm		
σ_{cr} [MPa]	331	301	288
F_{cr} [kN]	24.9	23.9	24.6
wall-thickness	t = 2.0 mm		
σ_{cr} [MPa]	587	533	510
F_{cr} [kN]	73.7	70.6	72.6
wall-thickness	t = 2.5 mm		
σ_{cr} [MPa]	914	828	791
F_{cr} [kN]	115.2	109.7	112.5
wall-thickness	t = 3.0 mm		
σ_{cr} [MPa]	1310	1184	1128
F_{cr} [kN]	198.7	188.3	192.6
number of half-waves	6	8	9

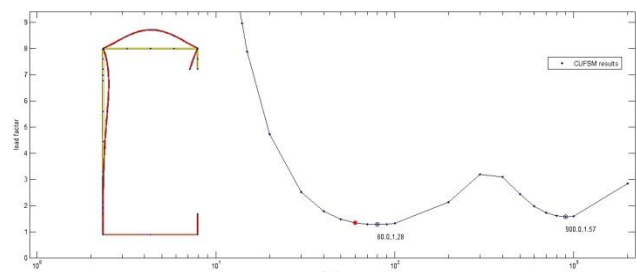


Fig. 6. Beam B1, $L = 500 \text{ mm}$: the relationship between the length of half-wave and load factor

3.3. The analysis of beam B2 - lipped flanges with perforated web

The cross-section of beam B2 with perforated web is presented in Fig. 7. The lipped flanges and perforated web improve the load capacity, strength and stability of beam with significantly reducing its weight too much. Perforation at length H is ten holes with a diameter of 9 mm. The dimension between the holes is 8 mm.

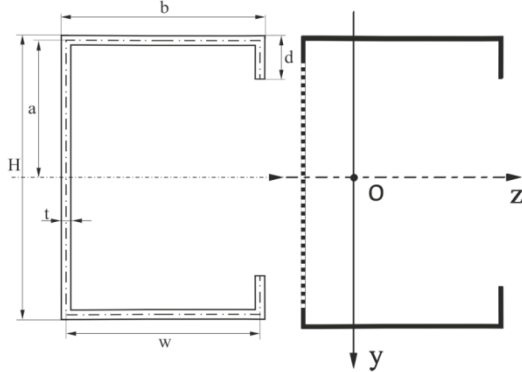


Fig.7. The cross-section of beam B2 with perforated web

The moment of inertia of beam B2 is equal to $J_y=92.8 \text{ cm}^4$ for the wall-thickness $t=0.6 \text{ mm}$, $J_y=123.8 \text{ cm}^4$ for the wall-thickness $t=0.8 \text{ mm}$, $J_y=154.7 \text{ cm}^4$ for the wall-thickness $t=1.0 \text{ mm}$, $J_y=170.2 \text{ cm}^4$ for the wall-thickness $t=1.1 \text{ mm}$, $J_y=185.7 \text{ cm}^4$ for the wall-thickness $t=1.2 \text{ mm}$, $J_y=194.5 \text{ cm}^4$ for the wall-thickness $t=1.25 \text{ mm}$, $J_y=232.1 \text{ cm}^4$ for the wall-thickness $t=1.5 \text{ mm}$, $J_y=309.5 \text{ cm}^4$ for the wall-thickness $t=2.0 \text{ mm}$, $J_y=386.9 \text{ cm}^4$ for the wall-thickness $t=2.5 \text{ mm}$ and $J_y=464.3 \text{ cm}^4$ for the wall-thickness $t=3.0 \text{ mm}$, respectively. The relationship between the load factor and length of half-wave and buckling mode of beam B2 (FSM) is shown in Fig. 8.

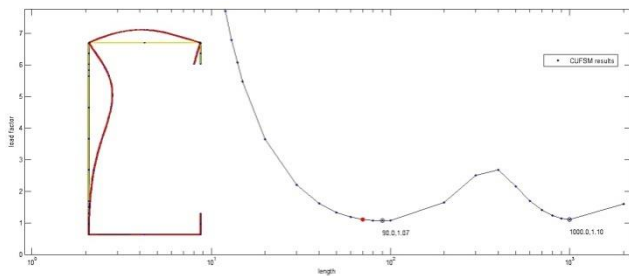


Fig.8. Beam B2, $L = 500 \text{ mm}$: the relationship between the length of half-wave and load factor

The calculated values of critical stresses / forces and the number of half-waves are presented in Tab. 3. The critical forces value slightly decreases for a beam with lipped flanges and with perforated web.

Tab.3. Beam B2, wall-thickness from $t=0.60 \text{ mm}$ to $t=3.00 \text{ mm}$: critical stresses and forces and the number of half-waves

L [mm]	400	500	600
wall-thickness	t = 0.6 mm		
σ_{cr} [MPa]	48	43	40
F_{cr} [kN]	1.4	1.4	1.4
wall-thickness	t = 0.8 mm		
σ_{cr} [MPa]	85	76	71
F_{cr} [kN]	3.4	3.2	3.2

wall-thickness	t = 1.0 mm		
σ_{cr} [MPa]	133	118	110
F_{cr} [kN]	6.6	6.3	6.3
wall-thickness	t = 1.1 mm		
σ_{cr} [MPa]	161	143	132
F_{cr} [kN]	8.0	7.6	7.5
wall-thickness	t = 1.2 mm		
σ_{cr} [MPa]	192	170	159
F_{cr} [kN]	11.5	10.8	10.9
wall-thickness	t = 1.25 mm		
σ_{cr} [MPa]	207	184	172
F_{cr} [kN]	12.9	12.2	12.2
wall-thickness	t = 1.5 mm		
σ_{cr} [MPa]	298	265	248
F_{cr} [kN]	22.4	21.1	21.2
wall-thickness	t = 2.0 mm		
σ_{cr} [MPa]	530	470	440
F_{cr} [kN]	66.6	62.3	62.6
wall-thickness	t = 2.5 mm		
σ_{cr} [MPa]	826	733	684
F_{cr} [kN]	104.1	97.1	97.3
wall-thickness	t = 3.0 mm		
σ_{cr} [MPa]	1187	1051	980
F_{cr} [kN]	180	167.1	167.3
number of half-waves	6	8	9

3.4. The analysis of beam B3 - sigma

The cross-section of beam B3 sigma is presented in Fig. 9. The stiffened web significantly improves the load capacity, strength and stability of beam without increasing its weight too much.

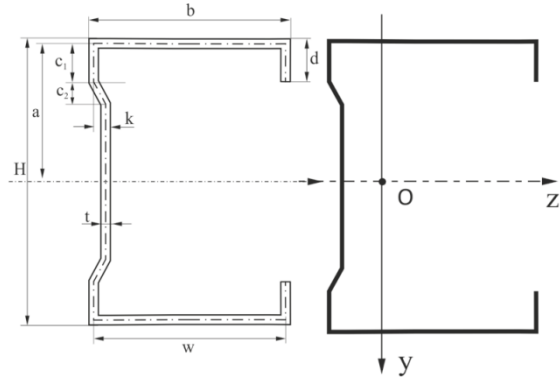


Fig. 9. The cross-section of beam B3 with stiffened web

The moment of inertia of beam B3 is equal to $J_y=93.9 \text{ cm}^4$ for the wall-thickness $t=0.6 \text{ mm}$, $J_y=125.2 \text{ cm}^4$ for the wall-thickness $t=0.8 \text{ mm}$, $J_y=156.6 \text{ cm}^4$ for the wall-thickness $t=1.0 \text{ mm}$, $J_y=172.2 \text{ cm}^4$ for the wall-thickness $t=1.1 \text{ mm}$, $J_y=187.9 \text{ cm}^4$ for the wall-thickness $t=1.2 \text{ mm}$, $J_y=195.7 \text{ cm}^4$ for the wall-thickness $t=1.25 \text{ mm}$, $J_y=239.9 \text{ cm}^4$ for the wall-thickness $t=1.5 \text{ mm}$, $J_y=313.2 \text{ cm}^4$ for the wall-thickness $t=2.0 \text{ mm}$, $J_y=391.5 \text{ cm}^4$ for the wall-thickness $t=2.5 \text{ mm}$ and $J_y=469.8 \text{ cm}^4$ for the wall-thickness $t=3.0 \text{ mm}$, respectively. The relationship between the load factor and length of half-wave and buckling mode of beam B3 (FSM) is shown in Fig. 10.

The calculated values of critical stresses/forces and the number of half-waves are presented in Tab.4. The wall-thickness increases the values of critical loads. In addition, the dimensions of the length of the middle span L section of the cross-section of the beams tested did not significantly affect the critical stress value or the half-wave number.

Tab. 4. Beam B3, wall-thickness from $t=0.60$ mm to $t=3.00$ mm: critical stresses and forces and the number of half-waves

L[mm]	400	500	600
wall-thickness	t=0.6 mm		
σ_{cr} [MPa]	55	51	52
F_{cr} [kN]	1.7	1.6	1.8
wall-thickness	t=0.8 mm		
σ_{cr} [MPa]	97	91	89
F_{cr} [kN]	3.9	3.9	4.1
wall-thickness	t=1.0 mm		
σ_{cr} [MPa]	153	143	140
F_{cr} [kN]	7.7	7.7	8.1
wall-thickness	t=1.1 mm		
σ_{cr} [MPa]	183	170	167
F_{cr} [kN]	10.2	10.0	10.6
wall-thickness	t=1.2 mm		
σ_{cr} [MPa]	218	202	198
F_{cr} [kN]	13.2	13.0	13.7
wall-thickness	t=1.25 mm		
σ_{cr} [MPa]	236	219	215
F_{cr} [kN]	14.9	14.7	15.5
wall-thickness	t=1.5 mm		
σ_{cr} [MPa]	339	313	306
F_{cr} [kN]	25.8	25.2	26.4
wall-thickness	t=2.0 mm		
σ_{cr} [MPa]	597	549	534
F_{cr} [kN]	75.9	73.6	76.9
wall-thickness	t=2.5 mm		
σ_{cr} [MPa]	925	845	818
F_{cr} [kN]	117.9	113.3	117.7
wall-thickness	t=3.0 mm		
σ_{cr} [MPa]	1318	1200	1157
F_{cr} [kN]	202.3	193.1	199.8
number of half-waves	6	8	9

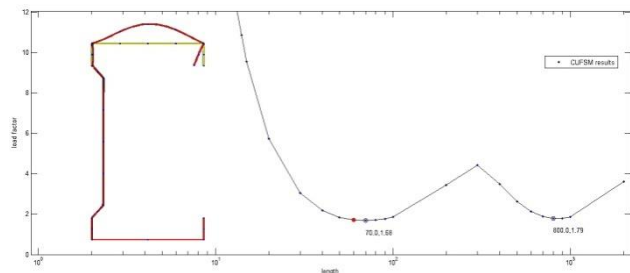


Fig.10. Beam B3 sigma with stiffened web, $L = 500$ mm: the relationship between the length of half-wave and load factor

3.5. The analysis of beam B4 - sigma with perforated web

The cross-section of beam B4 with perforated web is presented in Fig. 11. The lipped flanges and perforated web improve the load capacity, strength and stability of beam with significantly reducing its weight too much. Perforation

at length H is ten holes with a diameter of 5 mm. The dimension between the holes is 3 mm.

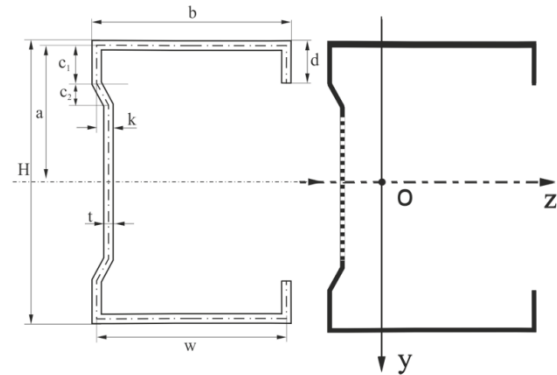


Fig. 11. The cross-section of beam B4 with stiffened and perforated web

The moment of inertia of beam B4 is equal to $J_y=93.9$ cm⁴ for the wall-thickness $t=0.6$ mm, $J_y=125.2$ cm⁴ for the wall-thickness $t=0.8$ mm, $J_y=156.6$ cm⁴ for the wall-thickness $t=1.0$ mm, $J_y=172.2$ cm⁴ for the wall-thickness $t=1.1$ mm, $J_y=187.9$ cm⁴ for the wall-thickness $t=1.2$ mm, $J_y=195.7$ cm⁴ for the wall-thickness $t=1.25$ mm, $J_y=239.9$ cm⁴ for the wall-thickness $t=1.5$ mm, $J_y=313.2$ cm⁴ for the wall-thickness $t=2.0$ mm, $J_y=391.5$ cm⁴ for the wall-thickness $t=2.5$ mm and $J_y=469.8$ cm⁴ for the wall-thickness $t=3.0$ mm, respectively. The relationship between the load factor and length of half-wave and buckling mode of beam B4 (FSM) is shown in Fig. 12.

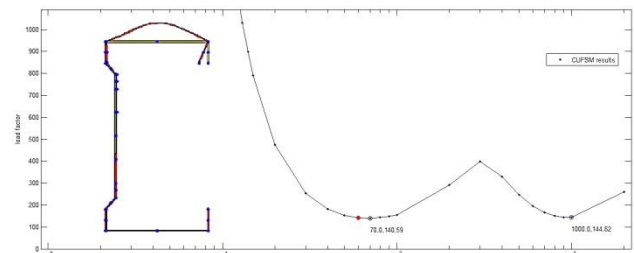


Fig.12. Beam 4 with perforated web, $L = 500$ mm: the relationship between the length of half-wave and load factor

The calculated values of critical stresses/forces and the number of half-waves are presented in Tab. 5. The critical forces value slightly decreases for a beam with lipped flanges and with perforated web. The weight of a thin-walled beam with a perforated web is significantly reduced.

Tab. 5. Beam B4, wall-thickness from $t=0.60$ mm to $t=3.00$ mm: critical stresses and forces and the number of half-waves

L[mm]	400	500	600
wall-thickness	t=0.6 mm		
σ_{cr} [MPa]	55	52	51
F_{cr} [kN]	1.7	1.7	1.8
wall-thickness	t=0.8 mm		
σ_{cr} [MPa]	98	92	91
F_{cr} [kN]	4.0	3.9	4.2
wall-thickness	t=1.0 mm		
σ_{cr} [MPa]	153	142	140
F_{cr} [kN]	7.7	7.6	8.1
wall-thickness	t=1.1 mm		

σ_{cr} [MPa]	186	172	169
F_{cr} [kN]	10.3	10.1	10.7
wall-thickness	t=1.2 mm		
σ_{cr} [MPa]	220	204	200
F_{cr} [kN]	13.4	13.1	13.8
wall-thickness	t=1.25 mm		
σ_{cr} [MPa]	236	219	214
F_{cr} [kN]	14.9	14.7	15.4
wall-thickness	t=1.5 mm		
σ_{cr} [MPa]	339	313	305
F_{cr} [kN]	25.8	25.2	26.3
wall-thickness	t=2.0 mm		
σ_{cr} [MPa]	597	547	532
F_{cr} [kN]	75.9	73.3	76.6
wall-thickness	t=2.5 mm		
σ_{cr} [MPa]	923	843	815
F_{cr} [kN]	117.7	113.0	117.3
wall-thickness	t=3.0 mm		
σ_{cr} [MPa]	1316	1196	1151
F_{cr} [kN]	202	192.4	198.8
number of half-waves	6	8	9

2.7. The analysis of beam B5-S with stiffened web

The cross-section of beam B5-S is presented in Fig. 13. The boxed flanges significantly improve the load capacity, strength and stability of beam without increasing its weight too much. Moreover, the stiffeners in the web make it stiffer and less prone to buckling.

The moment of inertia of beam B5-S is equal to $J_y=193.5 \text{ cm}^4$ for the wall-thickness $t=0.6 \text{ mm}$, $J_y=258.0 \text{ cm}^4$ for the wall-thickness $t=0.8 \text{ mm}$, $J_y=322.5 \text{ cm}^4$ for the wall-thickness $t=1.0 \text{ mm}$, $J_y=354.8 \text{ cm}^4$ for the wall-thickness $t=1.1 \text{ mm}$, $J_y=387.1 \text{ cm}^4$ for the wall-thickness $t=1.2 \text{ mm}$, $J_y=403.2 \text{ cm}^4$ for the wall-thickness $t=1.25 \text{ mm}$, $J_y=483.8 \text{ cm}^4$ for the wall-thickness $t=1.5 \text{ mm}$, $J_y=645.1 \text{ cm}^4$ for the wall-thickness $t=2.0 \text{ mm}$, $J_y=806.4 \text{ cm}^4$ for the wall-thickness $t=2.5 \text{ mm}$ and $J_y=967.7 \text{ cm}^4$ for the wall-thickness $t=3.0 \text{ mm}$, respectively. The relationship between the load factor and length of half-wave and buckling mode of beam B5-S (FSM) is shown in Fig. 14.

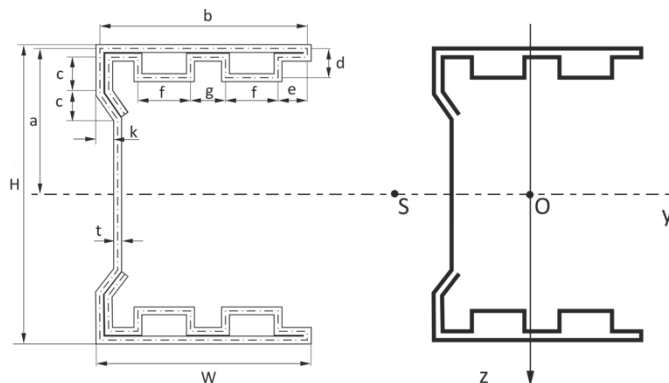


Fig.13. The cross-section of beam B5-S - double box flanges

The calculated values of critical stresses / forces and the number of half-waves are presented in Tab.6. Stiffened web and double box flanges significantly increase the beams

resistance to local buckling. Double box flanges, significantly affect the beams resistance to local buckling. It is the best of non-standard beam of all the thin-walled, cold-formed channel beams presented in this paper.

Tab. 6. Beam B5-S, wall-thickness from $t=0.60 \text{ mm}$ to $t=3.00 \text{ mm}$: critical stresses and forces and the number of half-waves

L[mm]	400	500	600
wall-thickness	t=0.6 mm		
σ_{cr} [MPa]	57	56	58
F_{cr} [kN]	3.5	3.7	4.1
wall-thickness	t=0.8 mm		
σ_{cr} [MPa]	102	99	103
F_{cr} [kN]	8.5	8.7	9.8
wall-thickness	t=1.0 mm		
σ_{cr} [MPa]	159	155	160
F_{cr} [kN]	16.5	17.1	19.0
wall-thickness	t=1.1 mm		
σ_{cr} [MPa]	193	187	193
F_{cr} [kN]	22.1	22.7	25.2
wall-thickness	t=1.2 mm		
σ_{cr} [MPa]	229	222	230
F_{cr} [kN]	28.6	29.4	32.7
wall-thickness	t=1.25 mm		
σ_{cr} [MPa]	251.2	243.1	251
F_{cr} [kN]	32.5	33.6	37.3
wall-thickness	t=1.5 mm		
σ_{cr} [MPa]	356	345	355
F_{cr} [kN]	55.7	57.2	63.2
wall-thickness	t=2.0 mm		
σ_{cr} [MPa]	629	607	621
F_{cr} [kN]	164.6	167.6	184.1
wall-thickness	t=2.5 mm		
σ_{cr} [MPa]	976	936	952
F_{cr} [kN]	256.3	258.5	282.3
wall-thickness	t=3.0 mm		
σ_{cr} [MPa]	1393	1330	1345
F_{cr} [kN]	440.3	440.8	478.5
number of half-waves	6	8	9

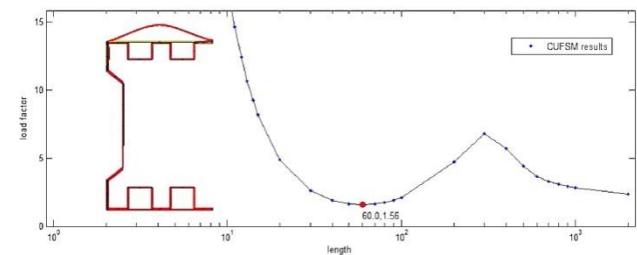


Fig.14. Beam B5-S, L = 500 mm: the relationship between the length of half-wave and load factor

An example influences of wall-thickness $t=1.00 \text{ mm}$ and $t=1.25 \text{ mm}$ on the relationship between load factor and the length of half-wave for beam B5 sigma is presented in Fig. 15.

It may be concluded that lipped flanges and web stiffeners improve the stiffness and stability of beams (Tab. 2-6). The critical forces increase slightly with the length of middle span L . However, parameter L in the considered range has virtually no influence on the critical stresses (less than

3%), but the longer is the middle span the more half-waves are observed. Other parameters such as wall-thickness and web stiffener have no influence on the number of half-waves.

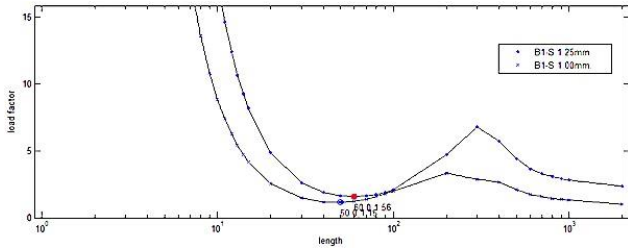


Fig. 15. Beam B5-S, $L = 500$ mm: the relationship between the length of half-wave and load factor

Numerical analyses make it possible to observe interaction between different buckling modes of flanges and the web. Moreover, they help to build more accurate analytical models. The obtained results justify the search for new, other than normalized cross-sections of cold-formed thin-walled beams.

4. CONCLUSIONS

The paper describes numerical investigations (FSM) of cold formed non-standard, thin-walled channel beams. Five different cross-sections of beams are examined. The beams are subjected to pure bending and their linear elastic stability and limit load are considered. The aim of the research is comparison of numerical results, obtained using CuFSM for all modified cross-sections. In that way models numerical simulating pure bending are validated. Numerical investigations make it possible to observe buckling modes of flanges and web including their interactions. This confirms that numerical simulations need to be done to prove if test stands simulating pure bending are built properly, e.g. where to place strain gauges. Moreover, they may give a better view on structure than actual tests. On the other hand, numerical model is based on some assumptions and simplifications. Therefore, numerical results should be compared in the future with experimental ones to validate them. In Fig. 16 the comparison of numerical (FSM) and experimental stresses are shown. They refer to all from five beams of wall-thickness from $t=0.60$ mm to $t=3.00$ mm.

Values of the critical forces presented in Fig. 16 confirm the need of numerical simulation (FSM) for non-standard C-Beams. There is visible conclusion that bend web (B3, B4, B5-V) strengthened the construction relative to beams without bend web in about 45% for wall-thickness $t=1.00$ mm and about 43% for wall-thickness $t=1.25$ mm. Values of the critical forces slightly increase with the length of the middle span L . Moreover, the length of the middle span L of analysed beams affected number of half-waves, i.e. for the length of the middle span L the number of buckling half-waves increases but it is not depending of beam's wall-thickness or strengthen along web.

Values of the critical forces slightly decrease for the beams with perforated web.

The presented investigations lead to the following conclusions:

- numerical investigations are supplementary to experimental tests and in some cases may even give better results, e.g. when critical forces and local buckling modes are difficult to measure,
- difference between numerical results (FSM) and experimental ones is small and less than 2% in the case of beam B1-V for wall-thickness $t=1.00$ mm,
- difference between calculated values of the critical forces for the beams with C-sections in case of the length of the middle span L amounted nothing above 13%,
- the band web influence significantly on value of critical forces between thin-walled channel beam with bend web and beams with stiffeners flanges,
- the length of the middle span L has no meaningful influence on value if the critical forces, however it has influence on numbers of half-waves, i.e. for the length of the middle span L the number of half-waves increases
- the number of half-waves is the same for beams with different wall-thickness, same cross-sections' shape and the same length of the middle span L is not depending of strengthen along web
- the results justify searching for new shapes of cross-section of cold-formed thin-walled beams that have not been included in standards.

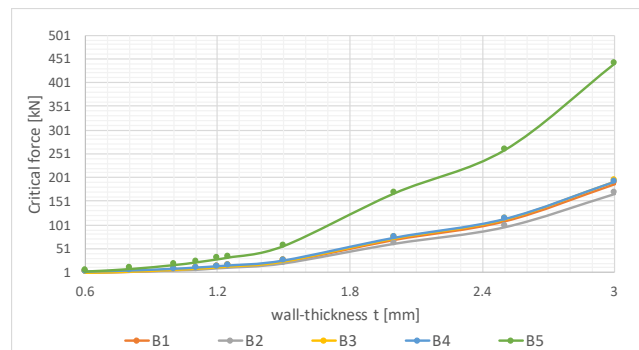


Fig. 16. Comparison between the results of critical forces for different wall-thickness, $L=500$ mm

In Tab. 7. the comparison of numerical (FSM) end experimental stresses is shown. They refer to beams B5-S of wall-thickness $t=1.00$ mm. In this case, numerical results seem to be a little bit lower 5.5% than experimental ones. Critical forces, numerical and experimental ones, are compared in Tab. 7. The difference between them is small 2.2%, but in contrast to stresses numerical results are higher than experimental ones [39].

Tab. 7. The comparison of experimental and numerical results (FSM), Beam B5-S, wall-thickness $t=1.00$ mm, $L=500$

Investigations	B5-S ($t=1.00$ mm)	
	Stresses [MPa]	Critical force [kN]
experimental	165	16.9
numerical	155	17.1
relative differences [%]	5.5%	2.2%

This work presents preliminary investigations done in order to better understand a problem and search for new, untypical shapes of the cross-sections of cold-formed thin-walled beams that could increase their strength and stability.

ACKNOWLEDGEMENTS

The project was funded by the National Science Centre allocated on the basis of the decision No. DEC-2017/25/B/ST8/00266 of 2017-11-23 – Contract No. UMO-2017/25/B/ST8/00266.

REFERENCES

- [1] **Ungureanu V., Dubina D.**, Sensitivity to Imperfections of Perforated Pallet Rack Sections, *Mechanics and Mechanical Engineering*, 17(2) (2013) 207–220.
- [2] **Rasmussen K.J.R., Hancock G.J.**, Geometric imperfections in plated structures subject to interaction between buckling modes, *Thin-Walled Structures*, 6 (1988) 433–452.
- [3] **SudhirSastry Y.B., Krishna Y., Budarapu P.R.**, Parametric studies on buckling of thin walled channel beams, *Computational Materials Science*, 96 (2015) 416–424.
- [4] **Bienias J., Gliszczynski A., Pjakubczak, Kubiak T., Majerski K.**, Influence of autoclaving process parameters on the buckling and postbuckling behaviour of thin-walled channel section beams, *Thin-Walled Structures*, 85 (2014) 262–270.
- [5] **Chen Y., Chen X., Wang C.**, Experimental and finite element analysis research on cold-formed steel lipped channel beams under web crippling, *Thin-Walled Structures*, 87(4) (2015) 1–52.
- [6] **Magnucki K., Paczos P.**, Optimal theoretical shape optimization of cold-formed thin-walled channel beams with drop flanges in pure bending, *Journal of Construction Steel Research*, 65 (2009) 1731–1737.
- [7] **Belingardi G., Scattina A.**, Experimental investigation on the bending behaviour of hybrid and steel thin walled box beams - The role of adhesive joints, *International Journal of Adhesion & Adhesives*, 40 (2013) 31–37.
- [8] **Biegus A., Czepizak D.**, Experimental investigations on combined resistance of corrugated sheets with strengthened cross-sections under bending and concentrated load, *Thin-Walled Structures*, 46 (2008) 303–309.
- [9] **Paczos P., Wasilewicz P.**, Experimental investigations of buckling of lipped, cold-formed thin-walled beams with I section, *Thin-Walled Structures*, 47 (2009) 1354–1362.
- [10] **Mahendran M., Jeyaragan M.**, Experimental investigation of the new built-up littesteel beams. Proc. 5th Int. Conference on Thin-Walled Structures, Vol.1, M. Mahendran (Editor) Queensland University of Technology, Brisbane, Australia, ICTWS, 18–20 June 2008, pp. 433–441.
- [11] **Magnucka-Blandzi E., Magnucki K.**, Buckling and optimal design of cold-formed thin-walled beams: review of selected problems, *Thin-Walled Structures*, 49 (2011) 554–561.
- [12] **Magnucka-Blandzi E., Paczos P., Wasilewicz P.**, Buckling study of thin-walled channel beams with double-box flanges in pure bending, Blackwell Publishing Ltd. Strain, An Intl Journal for Experimental Mechanics, 48 (2012) 317–325.
- [13] **Magnucki K., Paczos P., Kasprzak J.**, Elastic buckling of cold-formed thin-walled channel beams with drop flanges, *Journal of Structural Engineering-ASCE*, 136(7) (2010) 886–896.
- [14] **Paczos P.**, Experimental and numerical (FSM) investigations of thin-walled beams with double-box flanges, *Journal of Theoretical and Applied Mechanics*, 51(2) (2013) 497–504.
- [15] **Paczos P.**, Experimental investigations of thin-walled C-beams with nonstandard flanges, *Journal of Constructional Steel Research*, 93 (2014) 77–87.
- [16] **Debski H., Kubiak T., Teter A.**, Experimental investigation of channel-section composite profiles behaviour with various sequences of plies subjected to static compression, *Thin-Walled Structures*, 71 (2013) 147–154.
- [17] **Kolakowski Z., Mania R.J.**, Semi-analytical method versus the FEM for analyzing of the local post-buckling of thin-walled composite structures, *Composite Structures*, 97 (2013) 99–106.
- [18] **Loughlan J., Yidris N., Jones K.**, The failure of thin-walled lipped channel compression members due to coupled local-distortional interactions and material yielding, *Thin-Walled Structures*, 61 (2012) 14–21.
- [19] **Luo Hong-Guang, Guo Yao-Jie, Ma Shi-Cheng**, Distortional buckling of thin-walled inclined lipped channel beams bending about the minor axis, *Journal of Constructional Steel Research*, 67 (2011) 1884–1889.
- [20] **Camotim D., Dinis P.B.**, Coupled instabilities with distortional buckling in cold-formed steel lipped channel columns, *Stability of Structures XIITH Symposium, Zakopane 7 –11 September 2009*, Technical University of Lodz, 13–32.
- [21] **Silvestre N., Camotim D.**, On the mechanics of distortion in thin-walled open sections, *Thin-Walled Structures*, 48 (2010) 469–481.
- [22] **Trahair N.S.**, Buckling analysis design of steel frames, *Journal of Constructional Steel Research*, 65 (2009) 1459–1463.
- [23] **Adany S., Schafer B.W.**, Buckling mode decomposition of single-branched open cross-section members via finite strip method: Derivation, *Thin-Walled Structures*, 44 (2006) 563–584.
- [24] **Magnucki K., Rodak M., Lewinski J.**, Optimization of mono- and anti-symmetrical I-section of cold-formed thin-walled beams, *Thin-Walled Structures*, 44 (2006) 832–836.
- [25] **Loughlan J., Yidris N.**, The post-local buckling mechanics and ultimate carrying capability of uniformly compressed thin-walled I-section struts and columns, *Stability of Structures, XIITH Symposium, Zakopane 7 –11 September 2009*, Technical University of Lodz, pp. 33–48.
- [26] **Magnucki K., Magnucka-Blandzi E.**, Variational design of open cross section thin-walled beam under stability constraints, *Thin-Walled Structures*, 35(3) 1999 185–191.
- [27] **Magnucki K., Monczak T.**, Optimum shape of the open cross section of thin-walled beams. *Engineering Optimization*, 32(3) (2000) 335–351.
- [28] **Magnucki K., Maćkiewicz M., Lewiński J.**, Optimal design of a mono-symmetrical open cross section of a cold-formed beam with sinusoidally corrugated flanges, *Thin-Walled Structures*, 44(5) (2006) 554–562.
- [29] **CEN, European Committee for Standardisation**, EN 1993-1-3: Eurocode 3 - Design of Steel Structures – Part 1-3: General rules – Supplementary rules for cold-formed members and sheeting, 2006.
- [30] **Adany S., Schafer B.W.**, Buckling mode decomposition of single-branched open cross-section members via finite strip method: Derivation, *Thin-Walled Structures*, 44 (2006) 563–584.
- [31] **Li Z., Schafer B.W.**, Application of the finite strip method in cold-formed steel member design, *Journal of Constructional Steel Research*, 66 (2010) 971–980.
- [32] **Beregszászi Z., Ádány S.**, The Effect of Rounded Corners of Cold-Formed Steel Members in the Buckling Analysis via the Direct Strength Method, *Proceedings of the twelfth International Conference on Civil, Structural and Environmental Engineering Computing*, Edited by: B.H.V. Topping, L.F. Costa Neves and R.C. Barros, 2009, Paper 36.
- [33] **Adany S., Joo A.L., Schafer B.W.**, Buckling mode identification of thin-walled members by using cFSM base functions, *Thin-Walled Structures*, 48 (2010) 806–817.
- [34] **Djafour M., Djafour N., Megnounif A., Kerdal D.E.**, A constrained finite strip method for open and closed cross-section members, *Thin-Walled Structures*, 48 (2010) 955–965.
- [35] **Chu T.X., Ye Z., Li L., Kettle R.**, Local and distortional buckling of cold-formed zed-section beams under uniformly distributed transverse loads, *International Journal of Mechanical Sciences*, 48 (2006) 378–388.
- [36] **Magnucka-Blandzi E., Paczos P., Wasilewicz P.**, Buckling Study of Thin-walled Channel Beams with Double-box Flanges in Pure Bending, *Strain*, 48(4) (2012) 317–325.

- [37] **Li Z., Schafer B.W.**, CUFSM open source: <http://www.ce.jhu.edu/bschafer/cufsm/>
- [38] **Schafer B.W.**, Designing Cold-Formed Steel Using the Direct Strength Method, 18-th International Specialty Conference on Cold-Formed Steel Structures, October 26-27, 2006, Orlando, Florida.
- [39] **Grenda M., Paczos P.**, Experimental investigation of thin-walled channel beams with bend web, 6th International Conference on Structural Engineering, Mechanics and Computation SEMC 2016, Cape Town, South Africa, SEMC 2016. Insights and Innovations in Structural Engineering, Mechanics and Computation, A. Zingoni (Ed.), Taylor & Francis Group, London, ISBN978-1-138-02927-9,1034-1037.